
SYNTHESIS, SPECTRAL, SOLID STATE ELECTRICAL CONDUCTIVITY AND BIOLOGICAL ACTIVITY STUDIES ON SOME THIAZOLINE - CYCLODIPHOSPH(V)AZANE METAL COMPLEXES

ABD-ELNASSER M. A. ALAGHAZ^A AND SALWA A. H. ELBOHY^B

^a-Department of Chemistry, Faculty of Science, Al-Azhar University (for Boys), Nasr City, Cairo, Egypt

^b-Department of Chemistry, Faculty of Science, Al-Azhar University (for Girls), Nasr City, Cairo, Egypt

Abstract

Aminocyclodiphosph(V)azane of thiazoline, III (1,3-diphenyl-2,4-bis(2-acetyl-2-thiazolinehydrazone)-2,2,4,4-tetrachlorocyclodiphosph(V)azane, reacts with stoichiometric amounts of transition metal salts such as Co(II), Ni(II), and Cu(II) to afford coloured complexes in a moderate to high yield. The structure of the isolated complexes was suggested based on elemental analyses, IR, molar conductance, UV-Vis, ¹H and ³¹P NMR, solid reflectance, magnetic susceptibility measurements and dark electrical conductivity of solid state. The solid state electrical conductivity obtained reveals that the ligand (III) and its metal complexes behave as semiconducting materials. Most of the prepared compounds showed high bactericidal activity and, in some cases, the complexes have higher bactericidal activity than the ligand.

Keywords: cyclodiphosph(V)azane metal complexes; electronic; IR; magnetic moment; electrical conductivity.

Address correspondence to A. M. A. Alaghaz, Chemistry Department, Faculty of Science (Boys), Al-Azhar University, Nasr-City, Cairo, Egypt.

E-mail: aalaghaz@hotmail.com

Introduction

In recent years, the structural feature of four-membered N₂P₂ ring compounds in which the coordination number of *P* varies from three to five have attracted considerable attention.^{1,2} Heterocycles with P-C, P-N, P-O, and P-S bonds, in addition to their great biochemical and commercial importance,^{3,4} play a major role in some substitution mechanisms as intermediates or as transition states.^{3,4} Also, some *P*-containing heterocycles had been found to be potentially carcinostatics³ among other pharmacological activities. The introduction of trivalent *P* centers in the ring enhanced the versatility of the heterocycles in complexing with both hard and soft metals. Since the trivalent *P* centers could stabilize transition metals in low oxidation states, such complexes could be potential homogeneous or phase-transfer catalysts in various organic transformations.³

In the present work, the interaction of 1,3-diphenyl-2,2,2,4,4,4-hexachlorocyclodiphosph(V)azane (**I**) with 2-acetyl-2-thiazoline hydrazone **II** derivative and its metal complexes have been achieved. The proposed structure for **III** is shown in Scheme 1.

Results And Discussion

The structure of the ligand (**III**) was elucidated by elemental analyses (Table I), IR, UV, ^1H and ^{31}P NMR spectra.

IR Spectra

The assignments of the important bands of the free ligand are given in Table II. The spectra reveal the characteristic bands of the $\nu_{\text{P-NH}}$ stretching vibrations of the ligand at 2622 cm^{-1} .⁵⁻⁶ The free ligand exhibits bands at 3165 and 1567 cm^{-1} due to ν_{NH} and $\nu_{\text{C=N}}$, respectively. The low energy position of the $\nu_{\text{C=N}}$ band could be attributed to its involvement in conjugation with the aromatic system. The medium-weak bands at 2991 and 3051 cm^{-1} are assigned to the aliphatic and the aromatic protons. The $\nu_{\text{P-Cl}}$ stretching vibration is observed at 502 cm^{-1} . The band at 1224 cm^{-1} was assigned to the $\nu_{\text{P-N}}$ stretching vibration. Bands appear in the range $1622\text{--}1409\text{ cm}^{-1}$ may be attributed to $\nu_{\text{C=C}}$ of the aromatic rings and attached compounds (**II**).⁵ Moreover, the IR spectra showed weak band at 1072 cm^{-1} due to the $\nu_{\text{C-S-C}}$ stretching vibration of 1027 cm^{-1} of the thiazoline ring.^{7,8} The weak band observed at 2929 cm^{-1} is due to aromatic C-H stretching vibrations.⁵

Electronic Spectra

The fact that the expected band at 272 nm ,⁹ characteristic for the delocalization of the nonbonding electrons on the nitrogen atoms within the phosphazo ring of the dimeric structure was observed in the spectrum of ligand(**III**), suggested the presence of the phosphazo ring. The bathochromically shifted band observed at 289 nm for the ligand relative to that of the dimer 1, 3-diphenyl-2,2,2,4,4,4-hexachlorocyclodiphosph(V)azane (**I**) is explained to be due to the replacement for one chlorine atom of each phosphorus atom by the 2-acetyl-2-thiazoline hydrazone. The new band observed at 350 nm is attributed to the $n\text{-}\pi^*$ transition of attached compound(**II**), which is absent in the corresponding dimer (**I**) and this is considered as an evidence for the ligand formation.

¹H- and ³¹P-NMR Spectrum

The ¹H-NMR spectrum of the ligand (III) showed the following characteristic proton signals at: δ (7.82 ppm, m) is assigned for aromatic protons Ar-H and abroad signal at δ (5.90 ppm, s) is assigned for N-H proton, which disappeared on the addition of D₂O due to the proton exchange. The signals at δ (2.63 ppm, t) and (1.99 ppm, s) can be assigned to the CH₂ and CH₃ protons, respectively. The ³¹P NMR of the ligand records a signal at δ = 25.4 ppm, which supports the phosphazo ring structure.

Metal Complexes

The chemical behavior of III towards transition-metal cations was our goal in this article. The metal cations selected for this purpose were Co(II), Ni(II), and Cu(II). When a mixture of one mole of III in acetonitrile was reacted with two moles of the metal salts in acetonitrile, a change in colour was observed and the corresponding complex compounds IVa-c were precipitated. The products IVa-c were purified by washing with acetonitrile, and gave elemental analysis compatible with the general formula [(MX_n)₂(III)], where M = Co(II) or Ni(II) (X = OCOCH₃, n = 2), and Cu(II) (X = Br, n = 2). Accordingly, the formed complexes follow the general equation:



The analytical data of the isolated complexes are listed in Table I.

In addition the proposed structures of the complexes of III is confirmed using different physico-chemical tools such as IR, molar ratio, conductometric titration molar conductance, UV-Vis, magnetic moment, solid state electrical conductivity and biological activity.

IR Spectra

The most characteristic IR spectral bands of the metal chelates together with those of the free ligand are collected in Table II. The IR spectra of the metal complexes show a shift to lower frequencies of both $\nu_{C=N}$ (thiazoline ring) and ν_{N-H} indicating that both the C=N (thiazoline ring) and NH groups coordinate via nitrogen atoms to the cations (Table II). Practically unchanged ν_{C-S-C} vibration at 1027 cm⁻¹ of the thiazoline ring^{7,8} indicates that the thiazoline ring does not coordinate to metal from the sulphur atom. Furthermore, the aliphatic and aromatic protons are not greatly affected upon complexation. In all metal complexes, there are

new medium to weak bands appeared at lower frequencies between 316–265 cm^{-1} were assigned to ν M-N and two bands at 547, 545 cm^{-1} were attributed to ν M-O for IV_a and IV_b respectively.¹⁰ The bands observed at 1460, 1575 cm^{-1} and 1465, 1605 cm^{-1} in both Co(II), and Ni(II)-complexes were assigned to $\nu_{\text{sym.OCO}}$ and $\nu_{\text{asym.OCO}}$, respectively, which indicated that the acetate groups coordinate as a monodentate to the central metal cation in Co(II) and Ni(II) complexes respectively.¹⁰ This is supported with the observed characteristic $\nu_{\text{M-O}}$ band.¹⁰ The characteristic bands corresponding to the $\nu_{\text{P-NH}}$, $\nu_{\text{P-N}}$ and $\nu_{\text{P-Cl}}$ which were associated with all the investigated complexes are collected in Table II.

Spectrophotometric Measurements of Solution Stoichiometry

The absorption spectra of the Co²⁺, Ni²⁺, and Cu²⁺ complexes are shown in Figure 1. The diagrams in Figure 2, consists of two linear portions intersecting at 1:2 [ligand]/[M²⁺], where M²⁺ corresponding to Co²⁺, Ni²⁺, and Cu²⁺ respectively, indicating the formation of 2M: 1L species.¹⁰

Conductometric Titration

In order to follow up the behaviour of the ligand in solution with Co (II), Ni (II), and Cu (II), we investigated these systems using conductometric titration method.¹⁰ In this method 25 ml (10⁻⁴M) of M(II) where M(II) is Co(II), Ni(II) and Cu(II) solution in absolute ethanol was titrated with (10⁻³M) in absolute ethanol of ligand solution at room temperature 25°C which represented in Figure 3. The curves were plotted between the conductance of the solution and the volume of ligand added. The results show that the break in the curve occurred when the 2: 1 (M: L) species are formed in solution. The conductance of the reaction mixture was increase continuously with complexes under investigation. The reason for increase in conductivity after 2: 1 (M: L) complexes forms may be due to the presence of the ligand in ionic form in the medium (ethanol) which arises the conductivity.

Molar conductance data

The molar conductance values in DMF at 25°C for the complexes were found to be in the range 7.85–18.30 $\Omega^{-1} \text{mol}^{-1} \text{cm}^2$. The relatively low values indicate the non-electrolytic nature of these complexes. This can be accounted for by the satisfaction of the bivalent of the metal by the acetate or bromide anions. This implies the coordination of the anions to the metal ion centers.

Magnetic and Electronic Spectral Studies

The electronic spectra of the free ligand exhibit bands at 350 and 284nm which could be assigned to $n-\pi^*$ and $\pi - \pi^*$ transitions respectively. On complexation, the lower-energy band is shifted to a red shift, while the transition $\pi - \pi^*$ is slightly shifted to a blue shift.

The room temperature magnetic susceptibility measurement of the green Co(II) complex, $[\text{Co}_2(\text{III})(\text{OCOCH}_3)_4]$ **IVa** gave magnetic moment value μ_{eff} of 4.02B.M./Co(II) corresponding to three unpaired electrons are expected for a weak field ligand. The electronic spectra of the Co(II) complex as nujol mulls and/or solution in ethanol were recorded in the range 280–900 nm. The spectra exhibit peaks at 705 nm region, which may be assigned to ${}^4\text{A}_2 \rightarrow {}^4\text{T}_1$ (p) (ν_3) and is consistent with the tetrahedral geometry.¹⁰ The peaks observed at 299 nm and 240 nm regions, were assigned to $n-\pi^*$ and $\pi - \pi^*$ transitions respectively.

The green Ni-complex, $[\text{Ni}_2(\text{III})(\text{OCOCH}_3)_4]$ **IVb** gives value μ_{eff} of 2.87B.M./Ni(II) which is indicative of two unpaired electrons. The electronic spectra of the Ni(II) complex IVb exhibit absorption band near 666 nm which may be attributable to the ${}^3\text{T}_1 \rightarrow {}^3\text{T}_1$ (p), weak bands observed on the high and low energy sides of the 666 nm band have been assigned to spin-forbidden bands.¹⁰

The Cu(II) complex, $[\text{Cu}_2(\text{III})(\text{Br})_4]$ **IVc** absorbs at 692 nm was assigned to ${}^2\text{B}_2 \rightarrow {}^2\text{E}$ transition. The bands observed in the range 426 nm were assigned to the charge transfer via $\text{L} \rightarrow \text{M}$ (Cu^{2+}). The observed band at 280 nm was attributable to $\pi-\pi^*$ the magnetic moment of the Cu(II)-complex of μ_{eff} value of 1.93 B.M./Cu(II) is in accord with one unpaired electron which is indicative to square planar structure.¹⁰ We propose that the coordination with metal ions occurs through the nitrogen of the NH and C=N (thiazoline ring) groups to the structure depicted in Scheme 2.

Solid state electrical conductivity

The temperature dependency of the electrical conductivity for samples was measured in the range of temperature 290–350K as shown in Figure 4. The plots suggest that there are two types of conduction channels contributing to the conductivity and the linearity in the two temperature regions, which indicate that σ in these regions exhibits activated behavior to the relation:

$$\sigma = \sigma_0 \exp(-\Delta E/kT) \quad (1)$$

where σ_0 is the pre-exponential corresponding to $1/T = 0$, E the activation energy for electron transfer and k the Boltzmann's constant. The parameters of electrical conductivity of the samples are obtained from Figure 4 and are collected in Table III:

(a) Figure 4 shows the Arrhenius dependence of the conductivity of the samples. It appears that σ does not follow Eq. (1) over the complete temperature range. It is well known that, at least two transport mechanisms are considered in disorder materials when a change is observed in the slope of the Arrhenius plot of σ as seen in Figure 4. One is transport by carriers excited beyond a mobility edge into extended states E_C (conduction band edge) or E_V (valence band edge) leading to an activated energy $E = E_C - E_F$ ($E_F - E_V$) at high temperatures. The other is the hopping of carriers between localized states near the Fermi energy level at lower temperatures.¹¹ The activation energy ΔE was calculated from the slope of the straight line and the pre-exponential factor σ_0 was obtained by extrapolating the $\ln \sigma$ line to the value corresponding to $1/T = 0$. The obtained values were given in Table III. The calculated value of ΔE alone does not provide any indication as to whether the conduction occurs in the extended states above the mobility edge or by hopping in the localized states.¹² According to Mott and Davis,¹¹ the values of σ_0 is in the range 103–104 S/cm in the extended states. A smaller value of σ_0 indicates the presence of a wide of localization and conduction by hopping in the localized state. Except for the first region of Co(II) sample, the calculated values for samples both ΔE and σ_0 suggest that electrical conduction takes place by hopping in the localized states in the band gap. These localized levels are formed because of disorder in structure of the samples and thus disorder affects conductivity character of the samples. The transport of electrons on localized energy bands is generally investigated by flux theory method. On the other hand, the electrons transport to conduction band with hopping which is a character of quantum. This character shows that the conductivity between localized energy levels takes place by tunneling phenomena.^{13, 14}

(b) When electrical conductivity (σ_{25}) of samples at room temperature are compared with each other, their conductivities are Co(II) > Ni(II) > Cu(II). This is due to chemical composition of samples, i.e. in fact, III ratio in feed is increased, and its effect on conductivity can be both positive and negative. The band gap (E_g) and activation energy (E_a) were decreased with increased III ratio, and it can be explained as follows: when the sample is prepared, the localized energy levels are converted from conduction band to energy band gap or from valence band to energy gap. As the composition ratio of sample is increased, the width of the localized levels is expanded and so, the band gap is smaller. It is seen that the Cu(II) sample has the lowest value of energy band gap and activation energy. So, we have developed low band gap copolymer, and its value is 1.79 eV.

(c) The activation energies derived from the Arrhenius type of temperature dependence of conductivity may be associated with the excitation energy for thermal generation of carriers. The excitation mechanism is as follows: activation energy correspond to the energy band gap (E_g) calculated from the optical absorption for intrinsic conduction (i.e. $E_g \approx 2E_a$) or to the distance between the donor level and conduction band edge for extrinsic n-type conduction, or to the distance between acceptor level and the valence band edge for p-type conduction.¹⁵ When the activation energy values are compared with optical band gap values determined from the optical measurements, it is seen that the activation energy values do not provide discussion in above and furthermore, the samples have disorder medium. Thus, the activation energy values of samples can be interpreted by a band model containing a partially occupied set of trap states near the center of the energy gap between the valence and conduction bands. Figure 4 represents the case in which impurity is not donors of carriers unless they have previously been occupied. The conductivity is extrinsic in both (I) and (II), and the change of slope reflects a change from (I) E_a1/kT to $E_a2/2kT$ caused by a change in the number of excited carriers¹⁴; less the total number of impurity levels N , less the total number of carriers N_e , in (I) $n < N - N_e$ and in (II) $n > N - N_e$. It is seen that the samples have two different activation energies. These two activation energies are associated with the intramolecular and intermolecular conductivity process. Particularly, the lower values of E_a are associated with the intermolecular conduction process, while the higher values are related to the intramolecular conduction process.¹¹ In these samples there are two stages in the movement of a current-carrier-motion within the macromolecule and passage from one macromolecule to another, that is, the intramolecular and intermolecular transfer of the current carrier.

Biological Activity

The disc diffusion method was used to measure the antimicrobial activity of these complexes.¹⁴The test compounds were dissolved in dimethylformamide (DMF) (2% w/v) and added at a concentration of 0.5ml/disc to Whatman number 3 filter paper, 5mm diameter. The antimicrobial activity of some of the prepared compounds of the type **III** and (**IV**_{a-c}) were examined with different species of gram-positive bacteria such as Staphylococcus albus and Staphylococcus aureus, and gram-negative bacteria such as Pseudomonas aeruginosa, Klebsiella and Escherichia coli. The tested compounds showed remarkable biological activity against different types of gram-positive and gram negative bacteria. The data obtained are summarized in Table IV.

Experimental

All chemicals used were of analytical reagent grade. They included $\text{Co}(\text{CH}_3\text{COO})_2 \cdot 4\text{H}_2\text{O}$, $\text{Ni}(\text{CH}_3\text{COO})_2 \cdot 4\text{H}_2\text{O}$, and CuBr_2 and phosphorus pentachloride supplied from BDH. All solvents used were dry benzene, acetonitrile, ethanol, dimethylformamide (DMF), and deuterated dimethyl sulfoxide (DMSO). The preparation of 2-acetyl-2-thiazoline hydrazone (II) was carried out according to the Barros-García method.¹¹

Microanalytical analysis of C, H, N, Cl and S were carried out and phosphorus was determined gravimetrically as phosphoammonium molybdate using the R. Voy method.¹⁶ Infrared spectra were recorded in the solid state on a Mattson 5000 FTIR spectrometer using KBr disc technique. The absorbances of solutions were measured in the UV/Vis range (200–800 nm) using Unicam spectrophotometer model UV 2-100 and 1 cm matched quartz cells. The ^1H NMR spectrum of the ligand was recorded on a Varian FT-290.90 MHz spectrometer in deuterated DMSO using TMS as an internal standard. ^{31}P NMR spectra were run, relative to external H_3PO_4 (85%), with a Varian FT-80 spectrometer at 365 MHz. Magnetic measurements were recorded by the Gouy method at room temperature using a magnetic susceptibility balance (Johnson Mathey), Alfa product, Model No. (MK). Diamagnetic corrections were calculated from Pascal's constants. The conductometric measurements in solutions were carried out using conductivity TDS model 72. Metal contents were determined by titration against standard EDTA after complete decomposition of the complexes with aqua regia in a Kjeldahl flask several times. The biological activity experiments were carried out at Bab Al-Sheria University Hospital (Al-Azhar Microbiology Laboratory University). Conductivity measurements were made on discs having 1 mm thickness of the complex (IVc) sandwiched between two copper electrodes. The conductivity cell used was the same as that reported before.¹⁷ The electrical conductivity was measured in the temperature range 320–420 K.

Preparation of Ligand

The solid of 2-acetyl-2-thiazoline hydrazone (II) (1.41 g, 0.01 mmol) was added in small portions to a well stirred solution of the 1,3-diphenyl-2,2,2,4,4,4-hexachlorocyclodiphosph(V)azane (I) (2.285 g, 0.005 mmol) in 100 ml acetonitrile over a half-hour period. After the complete addition, the reaction mixture was heated under reflux for 2 h with continuous stirring. After completion of the reaction (HCl gas ceased to evolve) the reaction mixture was filtered while hot and the filtrate was left to cool at room temperature.

The obtained yellow solid was filtered off washed several times with acetonitrile, and dried in vacuo to give the corresponding 1,3-diphenyl-2,4-bis(2-acetyl-2-thiazoline hydrazone)-2,2,4,4-tetrachlorocyclodiphosph(V)azane (III) (Scheme 1).

Preparation of Complexes

A hot solution (60°C) of the metal salts [Co(OCOCH₃)₂.4H₂O (0.498 gm; 0.002 mole)], [Ni(CH₃COO)₂.4H₂O (0.497; 0.002)] or [CuBr₂ (0.466; 0.002)] in 50 ml acetonitrile was added dropwise to a hot solution of 1,3-diphenyl-2,4-bis(2-acetyl-2-thiazoline hydrazone)-2,2,4,4-tetrachlorocyclodiphosph(V)azane (III) (0.670 gm; 0.001 mole) in 100 ml acetonitrile in 2: 1 metal-to-ligand molar ratio at room temperature with continuous stirring. After complete addition of the hot metal-salt solution, the reaction mixture was heated under reflux for about two hours under dry conditions. The complexes obtained were washed with acetonitrile then with dry diethyl ether and dried in vacuo. The analytical data of both ligand and its metal complexes are listed in Table I.

Conclusion:

From the above results the new ligand "1,3-diphenyl-2,4-bis(2-acetyl-2-thiazoline hydrazone)-2,2,4,4-tetrachlorocyclodiphosph(V)azane" (III) form (2M: 1L) complex with the Co(II), Ni(II) and Cu(II) metal cations. The Co and Ni complexes of this ligand have tetrahedral structure, while the Cu complex has square-planar structure.

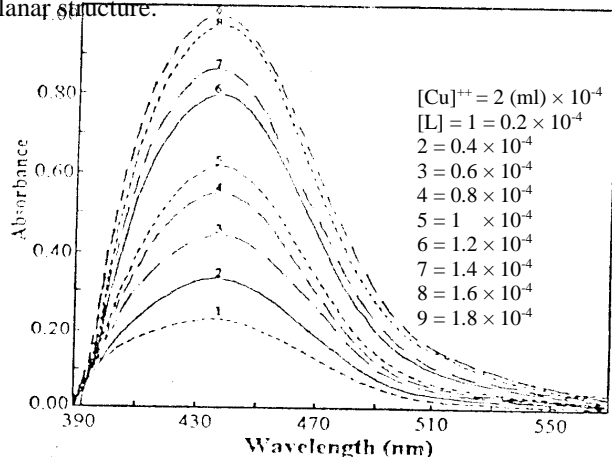


Figure 1. Absorption spectra of cu(ii)- iii complex, molar ratio method.

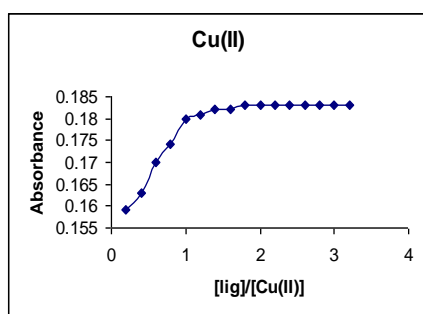


Figure 2. Results of molar ratio method for Cu(II)- iii complex.

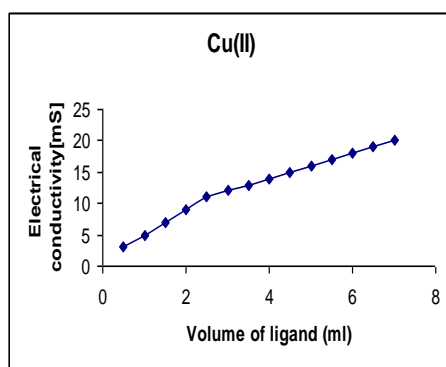
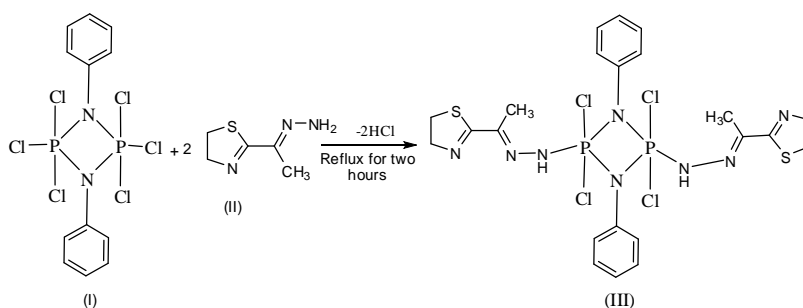
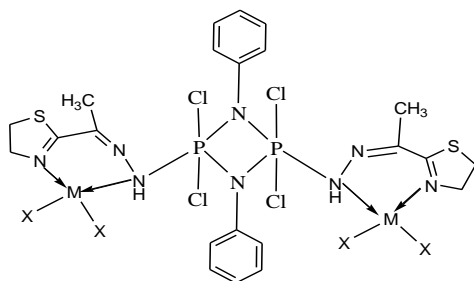


Figure 3. Conductometric titrations for Cu(II) with ligand (iii).



Scheme 1. Structure of ligand **III**: 1,3-di-phenyl-2,4-bis(2-acetyl-2-thiazoline hydrazone)-2,2,4,4-tetrachlorocyclodiphosph(V)azane.



Scheme 2. The proposed structure of the metal Complexes IVa-c. Where M = Co^{2+} , Ni^{2+} or Cu^{2+} , and X= acetate or bromide.

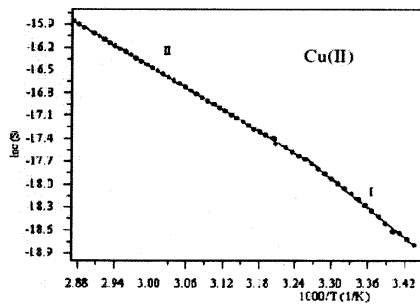
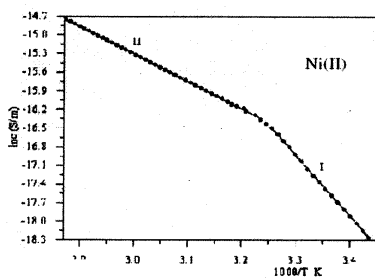
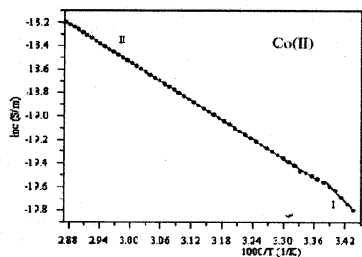


TABLE 1: Elemental analyses, yields, colours and melting points of ligand (III) and its corresponding metal complexes.

Comp. No.	M.F. (M.Wt)	M.p. (°C)	Color	Yield (%)	Elemental analyses Found (Calc.), %						
					C	H	N	P	Cl	S	M
III	C ₂₂ H ₂₆ Cl ₄ N ₈ P ₂ S ₂ (670.38)	198	Yellow	90.2	39.40 (39.42)	3.83 (3.91)	16.65 (16.71)	9.22 (9.24)	21.03 (21.15)	9.68 (9.57)	-
IVa	C ₃₀ H ₃₈ Cl ₄ Co ₂ N ₈ O ₈ P ₂ S ₂ (1024.43)	>360	Green	92.8	35.13 (35.17)	4.03 (3.74)	10.64 (10.94)	5.83 (6.05)	13.37 (13.84)	6.00 (6.26)	11.50 (11.51)
IVb	C ₃₀ H ₃₈ Cl ₄ Ni ₂ O ₈ P ₂ S ₂ (1023.95)	>360	Brown	92.7	35.03 (35.19)	3.93 (3.74)	10.36 (10.94)	6.00 (6.05)	13.35 (13.85)	6.02 (6.26)	11.43 (11.46)
IVc	C ₂₂ H ₂₆ Br ₄ Cl ₄ Cu ₂ N ₈ P ₂ S ₂ (1117.09)	>360	Brown	97.6	23.30 (23.65)	2.24 (2.35)	9.67 (10.03)	5.50 (5.55)	12.49 (12.69)	5.21 (5.74)	11.20 (11.38)

TABLE II: IR Spectra (4000–400 cm⁻¹) of III and its Complexes.

Compd. No.	$\nu(\text{NH})$	$\nu(\text{P-NH})$	$\nu(\text{P-N})$	$\nu(\text{P-Cl})$
III	3165br	2622w	1224m	502m
IVa	3122br	2600v.w	1222m	556sm
IVb	3124br	2600 v.w	1221m	464sm
IVc	3131m	2600 v.w	1221m	464m

m = Medium, w = Weak, vw = Very weak, br = Broad

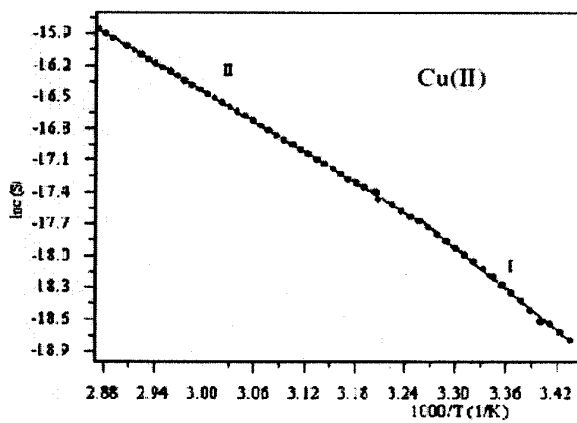
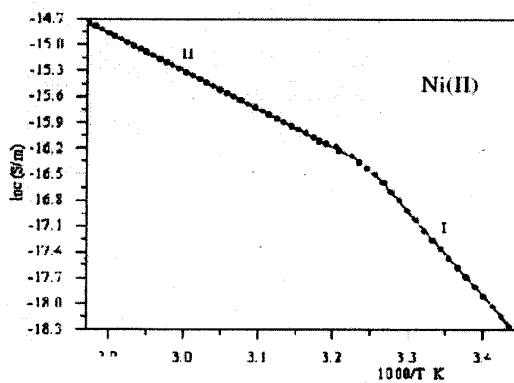
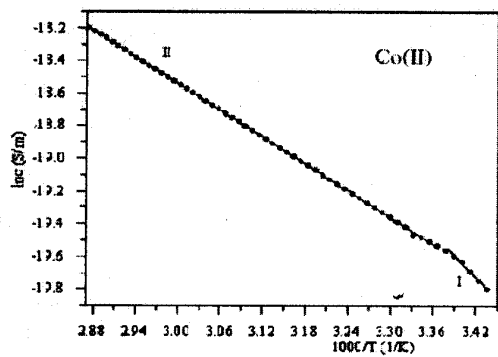
TABLE III: Values of the electrical conductivity (σ) and thermal activation energy of Co(II), Ni(II) and Cu(II) complexes.

Parameter	Co(II)	Ni(II)	Cu(II)
$\Delta E(\text{eV})$			
Region I	0.85	0.54	0.38
Region II	0.37	0.36	0.23
$E_g(\text{eV})$	3.26	3.14	1.79
$\sigma_0(\text{S/m})$			
Region I	6.74×10^6	29.85	1.23×10^{-2}
Region II	0.12	0.11	3.20×10^{-5}
$\sigma_{25}(\text{S/m})$	2.4×10^{-8}	1.14×10^{-8}	3.36×10^{-9}

TABLE IV: Antibacterial activity of the ligand (III) and corresponding metal complexes (IV_a-IV_c).

Comp d No.	Gram +ve		Gram -ve		
	<i>Staphylococcus albus</i>	<i>Staphylococcus aureus</i>	<i>Pseudomonas aeruginosa</i>	<i>Klebsiella Bacillus</i>	<i>Escheric hia coli</i>
III	+++	+++	++	+++	+
IV_a	+++	R	+++	+++	++
IV_b	R	++	R	+	R
IV_c	R	R	R	R	R

R = Resistance ++ = Moderately active, + = Less active +++ = Very active.



References

1. S. DEVARAJAN , S. MARAVANJI , BALAKRSHNA AND T.M JOAL, *Tetrahedron Letters*, 48 , 2283 (2007).
2. M. GJIKAJ, AND W. BROCKNER, *Vibrational Spectroscopy*, 39, 262 (2005).
3. M. CHAKRAVARTY, P. KOMMANA, AND K. C. KUMARA SWAMY, *Chem. Commun.* 5396 (2005).
4. M. S. BALAKRISHNA, R. PANDA AND J. T. MAGUE, *Inorg. Chem.*, **40**, 5620 (2002).
5. S. PRIVA, M. S. BALAKRISHNA, J. T. MAGUE AND S. M. MOBIN, *Inorg. Chem.*, **42**, 1272 (2003) .
6. M. L. LARSSON, AND A. HOLMGREN, *Vibrational Spectroscopy*, 34, 243 (2004).
7. N. SINGH , S. GUPTA, AND R. K. SINHA, *Inorg. Chem. Comm.*, 6, 416 (2003).
8. B. K. SINGH, R. K. SHARMA, AND B. S. GARG, *Spectrochimica Acta Part A*, 63, 96 (2006).
9. N. T. MADHU, P. K. RADHAKRISHNAN, AND W. LINER, *Journal of Thermal Analysis and Calorimetry*, 84(3), 607 (2006).
10. C. SHARABY, AND S.A. HASSAN, *Al- Azhar Bull Sci* 17 , 1 , 171 (2006).
11. M. ABD-ELLAH, B. A. EL-SAYED, M. A. EL-NAWAWY, AND A. M. A. ALAGHAZ *J. Phosphorus, Sulfur, and Silicon, and The Related Elements*, **177**, 2895 (2002).
12. R. S. FARAG, S. M. SHAABAN, B. A. EL-SAYED, I. M. ABD-ELLAH AND A. M. A. ALAGHAZ *Al-Azhar Bull. Sci.*, **15(1)**, 283 (2004).
13. N. SINGH , AND R. K. SINHA, *Inorganic Chemistry Communications*, 6, 97(2003).
14. N. SINGH , AND R. K. SINHA, *Inorganic Chemistry Communications*, 5, 255 (2002).
15. E. GHIDINI, M. DELCANALE, R. DE FANTI, A. RIZZI, M. MAZZUFERI, D. RODI, M. SIMONATO, B. MILCO LIPRERI, F. BASSANI, L. BATTIPAGLIA, M. BERGAMASCHIA, AND G. VILLETTI, *Bioorganic & Medicinal Chemistry*, **14**, 3263–3274 (2006).
16. F. J. BARROS-GARCÍA, A. BERNALTE-GARCÍA, F. LUNA-GILES AND M. A. MALDONADO-ROGADO, E. Viñuelas-Zahínos , *Polyhedron*, **24**, 1125-1132 (2005)
17. R. VOY, *Chem. Ztg. Chem. Apparatus*, **21**, 441 (1897).
18. M. A. AHMED AND F. A. RADWAN, *J. Phys. Chem. Solids*, **49**, 1385 (1988).